IAC-20-C1.3.14

FORMATION FLYING L-BAND APERTURE SYNTHESIS: DESIGN CHALLENGES AND INNOVATIVE FORMATION ARCHITECTURE CONCEPT

Francesca Scala
Politecnico di Milano, Milan, Italy, francesca1.scala@polimi.it

Gabriella Gaias
Politecnico di Milano, Milan, Italy, gabriella.gaias@polimi.it

Camilla Colombo
Politecnico di Milano, Milan, Italy, camilla.colombo@polimi.it

Manuel Martìn-Neira
ESA-ESTEC, Noordwijk, The Netherlands, Manuel.Martin-Neira@esa.int

It is well known that global maps of soil moisture and sea surface salinity are required to improve meteorological and climate prediction, as demonstrated by the Soil Moisture and Ocean Salinity (SMOS) satellite flying since 2009. In the context of future L-band missions for land and oceans applications, the spatial resolution should increase from 40 km, as for SMOS, to 1-10 km. Such improvement in the resolution of a radiometer is typically obtained increasing the aperture size: formation flying is envisioned as a potential way to achieve that spatial resolution.

This paper presents the results of the formation flying design and trade-off analysis. It shows the selection of the baseline geometry for the Formation Flying L-band Aperture Synthesis (FFLAS) mission concept, proposed by the European Space Agency. FFLAS foresees the use of three SMOS-like satellites, flying in a tight - rigid - formation in the low Earth orbit region. Starting from the scientific mission requirement of the L-band interferometer, an analysis, for possible three satellite planar formation flying architectures, has been carried out in the local orbital frame. For the sake of generality, a yaw angle is introduced to parametrise the possible orientation of the virtual instrument into the local orbital frame. The selection of the proper yaw angle, with respect to the transversal direction, is performed for fuel consumption balancing and optimisation. It also affects the sun-angle in the satellites' body-fixed frame, which is essential for solar panels dimensioning. Furthermore, the selection of the yaw angle is essential to evaluate the along-track and cross-track displacements, influencing the control effort and the inter-satellite collision risk. An established methodology to ensure collision avoidance for neighbouring satellites exploits the eccentricity and inclination separation between the spacecraft. The design investigates the possibility to implement such safety policies with the baseline formation flying geometry. The paper presents the outcome of these trade-off analyses. Results are obtained leveraging the Hill-Clohessy-Wiltshire formulation with the relative orbital elements environment, to include the effects of orbital perturbations and to assess the formation safety more straightforwardly.

I. INTRODUCTION

The Formation Flying L-band Aperture Synthesis mission (FFLAS) concept aims at increasing the spatial resolution of L-band imaging. Increasing the resolution up to 1-10 km can significantly improve the quality of land and oceans imaging for soil moisture and sea salinity analysis[1]. These high-quality observations lead to better meteorological and climate prediction. The FFLAS is currently under phase-A study conducted by Airbus Defence and Space and Politecnico di Milano, under a European Space Agency contract.

The idea of the mission concept starts from the Soil Moisture and Ocean Salinity (SMOS) mission. This single-satellite mission achieved a 40 km imaging resolution. Thus, the presented study takes advantage of the basic parameter for the L-band payload, resulting from the lesson learnt of the SMOS mission[2]. The increase of the aperture size is envisioned through a three-satellite formation flying, mounting the L-band aperture synthesis interferometer. The beneficial effect of exploiting formation flying to increase the virtual aperture of the instruments was widely studied[3,4].

The FFLAS phase-A mission concept is based on three L-band satellites in Low Earth Orbit (LEO), with a fixed – rigid – nominal formation configuration, lying on a plane orthogonal to the position vector. The L-band aperture synthesis interferometer is selected as a hexagonal array, of about 7 m in diameter, a slightly smaller size than SMOS one[5]. The centres of each

satellite in the formation are placed at the vertices of an equilateral triangle of about 13 m sides. Such formation would be equivalent to an aperture of 21 m diameter, achieving 9 km nadir resolution with an effective sensitivity better than SMOS. The preliminary mission analysis design was presented in a previous work[6].

The main objective of the work presented in this paper is to optimise the formation flying geometry to minimise the effect of the orbital perturbations. Specifically, according to the scientific mission requirements, the equilateral triangle must remain fixed and rigid during the nominal operation of the mission. The only degree of freedom for the design is given by the orientation of this triangle in the formation plane, defined as the yaw angle γ. The requirement of maintaining a fixed relative position among the satellites requires some forced motion to counterbalance the natural unperturbed relative dynamics. The control is needed to maintain the equilateral triangle formation geometry during the operations.

The additional control cost related to the effect of the orbital perturbations can be minimised by initialising the formation at convenient values of the mean argument of latitude of the reference orbit. The major perturbation for the relative dynamics in the considered orbital scenario, is the action of the non-homogeneous distribution of the mass of the Earth, as confirmed by the flight data analysis of the PRISMA formation-flying mission which operated in a very similar orbit environment[7].

The relations between the Hill-Clohessy-Wiltshire (HCW) solution and Relative Orbital Elements (ROEs)[8] and the form of the closed-form state-transition-matrix for the perturbed relative motion[9] is exploited to minimise the mean effect due to J_2. Moreover, the out-of-plane displacement δN is related to the relative inclination vector, and it is studied to analyse the fuel-balancing for the formation. Selecting a yaw angle that allows the balance of the propellant consumption among the satellites is fundamental for the design of the satellite platform. The three spacecraft will be identical, making important a similar fuel consumption during the nominal operations.

The analyses presented in the paper envision both the minimisation and the balancing of the delta-v budget. The latter is achieved performing an accurate analysis of the along-track and cross-track displacement, coupled with the initial argument of latitude. In addition to the reference formation geometry, both normal and radial displaced orbit are considered for the delta-v budget.

The yaw angle γ trade-off analysis is correlated with considerations on the Sun illumination, as well as on the self-shadowing and self-impingement analyses. The considerations on the Sun illumination are driven by the yearly and daily evolution of the Sun-satellite vector. For a Sun-Synchronous orbit, the angle between the normal to the orbit and the Sun is fixed in time, but the daily evolution of the spacecraft on it orbit produces a sinusoidal variation to the incidence angle on the solar panels. This analysis is carried out in parallel with the design of the solar panels for the platform.

Finally, the considerations on the self-impingement effect due to the on-board thruster are of great importance for the assessment of possible secondary effects on the optical and electronic devices on-board. Specifically, the formation is equipped with a low thrust electric engine. Such thrusters produce an ion discharge, that can erode the external part of the satellites. This kind of engine is selected since the ion thruster is particularly well suited for a range of applications, including constellations, in-orbit servicing, debris removal platforms or bespoke institutional missions such as GOCE[10].

The paper is organised as follow. Section II. provides an introduction on the Hill orbital frame[11], describing the formation geometry in the radial-transversal-normal frame.

Section III. introduces the relative orbital elements framework, providing the dynamical model used to propagate the relative motion. The state-transition matrix is given in the relative orbital elements framework, including the mean J_2 disturbance for a proper description of the natural evolution of the formation[7].

Section IV. presents the trade-off analyses for the admissible formation flying geometries:

i. Analysis of the initial argument of latitude, to minimize the J2 effect in the evolution.
ii. Analysis of the displacement in normal direction for a balanced formation in the tangential-normal plane. The control accelerations are defined via forced HCW solution, with no J_2 effect.
    The output of the analysis id the definition of the delta-v budget for different formation configurations.
iii. Analysis of the Satellite-Sun vector direction and the self-shadowing among the satellites.
    The output is the identification of the preferable yaw angle to minimise the self-shadowing effect.
iv. Analysis of the self-impingement effect, due to the ion thruster.
    The output is the selection of the better formation configuration in terms of the yaw angle, to minimise the possible secondary effect of the thruster plume, in relation to the main firings in the normal direction.

Section V reports the final formation geometry selection, according to the trade-off analyses results.

Finally, section VI provides a preliminary analysis on the formation safety, based on the selected configuration. The inter-satellite collision risk is assessed evaluating both the three-dimensional and the two-dimensional distance in the Radial-Tangential-Normal (RTN) frame.

II. HILL ORBITAL FRAME

The relative motion of a formation flying is typically described in the Hill Orbital Frame, via the HCW equations of motion[11]. This frame is defined by a unit vector triad $\{e_R, e_T, e_N\}$:

i. e_R is in the radial direction outward,
ii. e_N is in the direction of the orbital momentum vector (out-of-plane),
iii. e_T completes the right-hand triad in the transversal direction, along the satellite motion.

When the reference orbit of the formation is a circular one, the transversal direction coincides with the tangential direction to the satellite motion. This is the case of the reference orbit for the formation flying mission under study, and for this case, the triad is called the RTN frame. The coordinates in this frame are x, y, z, respectively.

The FFLAS orbit is selected like the SMOS orbit: an SSO at 775 km of altitude, with a Local Time of the Ascending Node (LTAN) at 6.00 am. The geometry of the SSO reference orbit is depicted in Fig. I, with respect to the line of nodes (J2000). It is shown how the selection of the LTAN results in a normal direction along the orbit angular momentum opposite to the Sun direction vector. This information is important for the sizing and allocation of the solar panels on-board the satellites.

During the nominal operations for the Earth Observation, the three satellites of the formation are placed at the vertex of an equilateral triangle of 13 m side. The generic baseline of the formation geometry is shown in Fig. II. The baseline triangle is centred at the origin of the RTN frame and has a generic orientation in the aperture plane (TN plane) defined by the γ angle, counter-clockwise. The three satellites are identified as $A, B,$ and C, and the circles represent the external diameter dimension of the spacecraft.

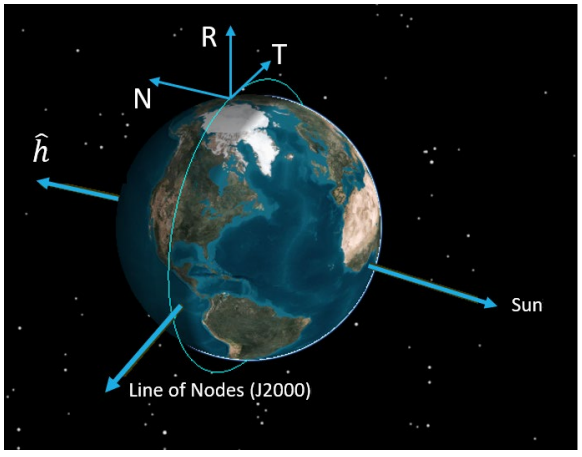

Fig. I: Reference Sun-Synchronous Orbit in the J2000 reference frame. The RTN frame is represented with the relative unit vector R, T, and N.

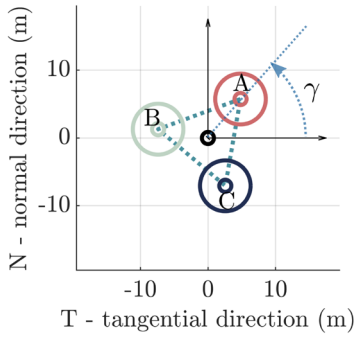

Fig. II: Formation flying geometry in the tangential-normal plane.

III. RELATIVE ORBITAL ELEMENTS FRAMEWORK

The natural motion of the formation flying is subjected to the external perturbations. For the case under analysis, the SSO is at 770 km of altitude. The most relevant perturbing effect for such condition is the Earth Oblateness[12], while the drag effect, the Solar Radiation Pressure (SRP) and the third body perturbation of the Moon and the Sun are considered negligible for the preliminary analysis presented in the followings. The drag effect for Low Earth Orbits (LEO) is important up to 500 km, while the SRP and the third body perturbation are order of magnitude lower than the primary J_2 effect[13].

The ROEs framework is introduced to describe the relative motion the three satellites of the formation. Differently form the classic HCW equations, the ROEs environment can easily include the effect of the mean J_2 orbital perturbation in the natural equations of motion.

The ROEs describe the orbital elements of each satellite in the formation with respect to the reference orbit. Considering the mean Keplerian elements of the reference SSO and of a generic satellite j of the formation as $\{a_C, e_C, i_C, \Omega_C, \omega_C, M_C\}$ and $\{a_C, e_C, i_C, \Omega_C, \omega_C, M_C\}$ respectively, the relative orbital elements are defined in Eq. [1] by $\delta\alpha$.

$$\delta\alpha = \begin{pmatrix} \delta a \\ \delta L \\ \delta e_x \\ \delta e_y \\ \delta i_x \\ \delta i_y \end{pmatrix} = \begin{pmatrix} a - a_c \\ u - u_c + (\Omega - \Omega_c)cosi_c \\ ecos\omega - e_c cos\omega_c \\ esin\omega - esin\omega_c \\ i - i_c \\ (\Omega - \Omega_c)sini_c \end{pmatrix} \quad [1]$$

where M is the mean anomaly, $u = \omega + M$ is the mean argument of latitude and δe and δi are the relative eccentricity and inclination vector, respectively.

The interpretation of the relative orbital elements with respect to the HCW equation is shown in Fig. III, where the ROEs are shown in terms of cross-track and along-track displacement.

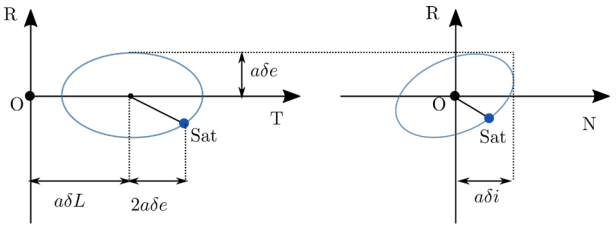

Fig. III: Interpretation of relative orbital elements in the RTN frame.

The natural evolution under the mean J_2 effect is described in term of variation of the ROEs for each satellite in the formation. This environment allows the description of the relative dynamics in terms of the State Transition Matrix (STM), including the contribution of the HCW classic equations and the mean J_2, as shown in Eq. [2]. The contribution due to the Earth oblateness is identified as the matrix components $\phi(i,j)$.

$$\begin{pmatrix} \delta a(t) \\ \delta L(t) \\ \delta e_x(t) \\ \delta e_y(t) \\ \delta i_x(t) \\ \delta i_y(t) \end{pmatrix} = \begin{bmatrix} 1 & 0 & 0 & 0 & 0 & 0 \\ \phi(2,1) & 1 & 0 & 0 & \phi(2,5) & 0 \\ 0 & 0 & 1 & \phi(3,4) & 0 & 0 \\ 0 & 0 & \phi(4,3) & 1 & 0 & 0 \\ 0 & 0 & 0 & 0 & 1 & 0 \\ \phi(6,1) & 0 & 0 & 0 & \phi(6,5) & 1 \end{bmatrix} \begin{pmatrix} \delta a(0) \\ \delta L(0) \\ \delta e_x(0) \\ \delta e_y(0) \\ \delta i_x(0) \\ \delta i_y(0) \end{pmatrix} \quad [2]$$

This representation allows to describe the $\delta\alpha$ at each time instant t, depending only on the initial conditions at the initial time. A first analysis is carried out to see whether there are some initial conditions that can minimise the effect of the mean J_2.

IV. ANALYSIS ON ADMISSIBLE FORMATION GEOMETRIES

IV.I Selection of the initial argument of latitude

A first analysis is performed on the initial argument of latitude u_0 to see if there are some conditions that minimise the effect of the J_2 perturbation. The study is parametrised in terms of the yaw angle γ and the initial argument of latitude u_0. The former defines the orientation of the formation in the TN plane, as shown in Fig. II, and can vary in the interval $[0,\ 2\pi]$. The latter describes the positioning of the reference virtual point of the formation along one orbit. It is computed starting from the ascending node of the orbit, where $u_0 = 0°$.

The effect of different argument of latitude and yaw angle is evaluated for each satellite in the ROEs environment. The analysis focuses on the variations in the eccentricity and inclination vector in time.

As from Eq. [2], the contribution of the mean J_2 is given by the matrix ϕ. This contribution adds to the non-forced unperturbed relative motion, given by the HCW dynamics. It generates sinusoidal oscillation on the natural motion. The aim of this analysis is to minimise this effect that influences the control effort of the formation, and, thus, to minimise the oscillation due to J_2. Specifically, the ROEs initial values that directly multiply the components of this matrix are easily given: $\delta a(0), \delta e_x(0), \delta e_y(0)$, and $\delta i_x(0)$.

For the mission under analysis, some considerations are valid at the initial time $t = 0$. First, due to the close formation nature requirement, the relative semi-major axis is considered negligible, for this preliminary analysis: $\delta a(0) = 0$. Moreover, the reference SSO and the orbits of the satellites are quasi-circular. For this preliminary analysis, the relative eccentricity vector is assumed negligible: $\delta e_x(0) = \delta e_y(0) = 0$. Finally, the only non-null initial relative element that multiplies the matrix ϕ, is the initial x-component of the inclination vector: $\delta i_x(0)$.

The aim of this first analysis is to select a combination of initial argument of latitude u_0 and yaw angle γ values such that the $\delta i_x(0)$ component is minimised. This results in the minimisation of the perturbation effect of the mean J_2 on the natural evolution of the formation. The results of the parametric analysis on δi_x for a generic satellite j in the formation ($j = A, B, C$) are shown in Fig. IV. The colormap shows in red and blue the areas with a combination of u_0 and γ resulting in a maximum modulus of δi_x; on the contrary, a δi_x with a null modulus is represented by the yellow area. In fact, the aim is to minimise the modulus of the inclination vector component, and from the Fig. IV the following situations can be identified.

i. For an angle γ of 0° or 180°, the inclination separation is null, independently form the argument of latitude.

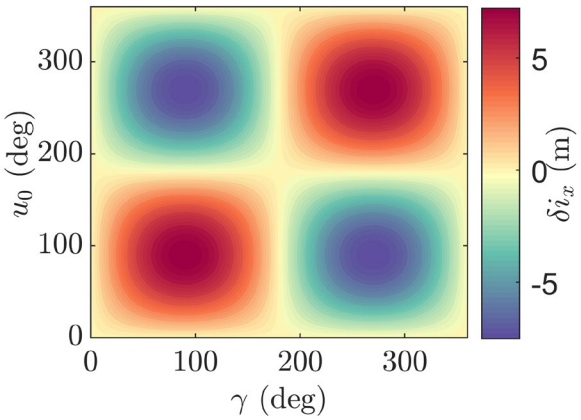

Fig. IV: Parametric analysis of the δi_x component, depending on the yaw angle γ and initial argument of latitude u.

ii. For a $u_0 = 0°$ or $180°$, the inclination separation is always null independently from the yaw angle γ. This situation corresponds to a formation flying initialised at the nodes.

iii. A $u_0 = 90°$ or $270°$, results in a sinusoidal variation of the initial inclination separation modulus, reaching the maximum value of the modulus in correspondence of $\gamma = 90°$ and $270°$.

As shown in Fig. II, the three satellites in the formation flying under analysis have an angular separation of $120°$. Now for the formation under analysis, selecting a $\gamma = 0°$ for the satellite $j = A$ results in a yaw angle for the spacecraft B and C of $120°$ and $240°$, respectively. Thus, the only condition that provides an initial null δi_x for all the three satellites is an initial argument of latitude at the nodes of the reference orbit: $u_0 = 0°$ or $180°$. The time propagation of the ROEs in such situation for the satellite j is reported in Fig. V, where it is shown how the relative orbital elements remain constant in time, resulting in an easier control from the formation maintenance point of view.

Thus, this first analysis set the initial argument of latitude for the nominal operations of the formation at the reference orbit nodes: $u_0 = 0°$ or $180°$.

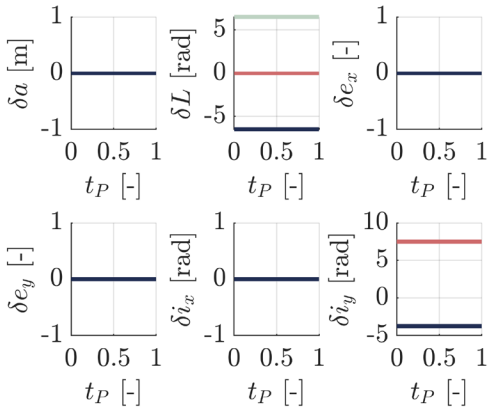

Fig. V: ROEs natural time evolution over one orbital period considering $u_0 = 0°$. The red, green, and blue line are the time evolution of the satellite A, B and C, respectively.

IV.II Fuel-Balanced formation analysis

The analysis, presented in this section, aims to study a formation configuration, compatible with the baseline in Fig. II, that ensure a balanced fuel consumption during the nominal operations of the mission. Initially, a parametric analysis on the yaw angle γ is performed to analyse the natural behaviour of each satellite j of the formation with respect to the virtual central point. The formation configuration is assumed as the baseline in Fig. II, with the reference virtual point at the centre of the equilateral triangle. Specifically, the key parameter to evaluate the propellant consumption during the nominal operation is the natural oscillation in the normal direction, δN. In fact, from mission requirements and safety considerations, the formation is required to stay rigid and the relative positions of each satellite fixed. The natural oscillations are evaluated in the RTN frame. The baseline formation under analysis lies on the transversal-normal plane and no oscillation in radial or transversal direction is present. Thus, to maintain the formation rigid, the δN shall be controlled during the nominal operation of the mission. The amplitude of such oscillation is proportional to the delta-v effort required to counteract it. For this reason, the aim of the analysis is to find a configuration in term of the γ angle, which provides similar oscillation amplitude for the three satellites. This situation results in a similar delta-v to control the satellite position, and therefore in a similar dimensioning in terms of propellant for the platform point of view.

The parametric analysis for the normal displacement δN is reported in Fig. VI. It shows two extreme formation configurations: FF-B1 represents a formation with a γ angle of $270°$, and FF-B2 represents a formation with a γ angle of $0°$. In the former situation, satellite A is subject to the maximum δN displacement, while satellite B and C undergo an equal non-null displacement. In the latter, instead, satellite A is subject to a null δN displacement, while satellite B and C undergo an equal non-null displacement, as in the previous condition.

The formation FF-B1 is a more balanced situation, even if delta-v difference would be present among satellite A and satellites B and C, due to the maximum δN of one satellite in the formation. On the other hand, a $\gamma = 0°$ is completely unbalanced since the satellite A needs no delta-v at all for the whole duration of the nominal operations.

This issue rises the need to study different formation configurations to balance the fuel consumption during the nominal operations. In the followings two analyses are presented, for N-displaced and R-displaced situation.

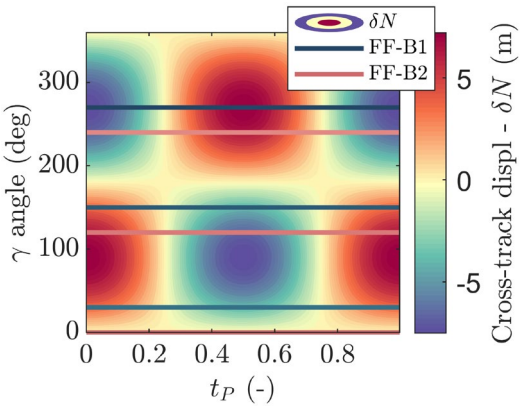

Fig. VI: Displacement in the cross-track direction over one orbit period parametrised on the yaw angle.

N-displaced orbits

A first strategy to realise the fuel-consumption balancing is to introduce a displacement in the normal direction ΔN, so that the formation equilateral triangle is no more centred in the origin of the RTN frame.

From the previous analysis on the baseline formation geometry, a γ yaw angle of 270° is preferred for the balancing in the normal direction. In fact, the FF-B1 configuration already provides a similar δN for the three satellites of the formation. Now the aim is to translate the formation along the N-axis to improve even more the situation. Specifically, the ΔN is chosen to have an equal displacement out-of-plane of all the three satellites of the formation.

The out-of-plane balanced configuration is depicted in Fig. VII. For the balancing, a $\Delta N = 1.875\,m$ is required, so that $|z_A| = |z_B| = |z_C|$. This provides a symmetric time evolution in the out-of-plane coordinate, as in Fig. VII: the same control on every satellite is required to counteract the natural oscillation along N.

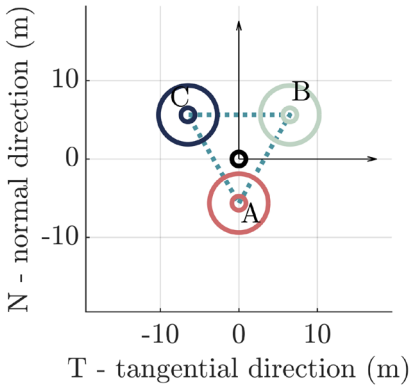

Fig. VII: N-displaced formation geometry, with a $\Delta N = 1.875$ m and $\gamma = 270°$.

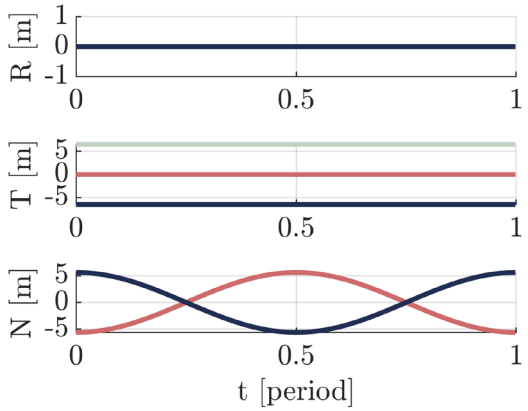

Fig. VIII: Time evolution over one orbit for the N-displaced geometry, with $u_0 = 0°$ and $\gamma = 270°$. The red, green, and blue line are the time evolution of the satellite A, B and C, respectively.

R-displaced orbits

A second analysis is introduced starting from the baseline formation and adding a displacement in the radial direction. A displacement in the radial direction ΔR is introduced for each one of the satellites to maintain a rigid planar formation in a plane orthogonal to the radial direction.

The analysis done considering a $\Delta R = 3$ m shows a non-constant evolution in both radial and tangential direction, differently from the previous result in Fig. VIII. This behaviour is reported in Fig. IX. As for the N-displaced orbit, a $\Delta N = 1.875$ m is introduced with the ΔR in the FF-B1 formation geometry.

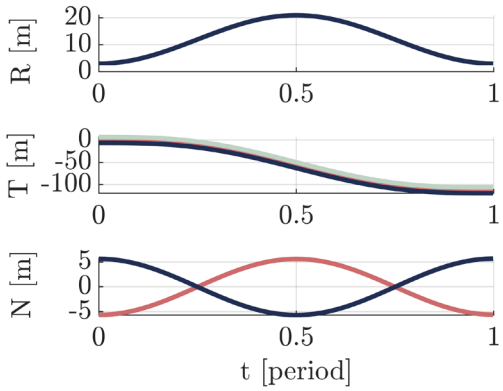

Fig. IX:Time evolution over one orbit for the N-displaced geometry, with u_0=0° and γ=270°. The red, green, and blue line are the time evolution of the satellite A, B and C, respectively.

Delta-v analysis

From the mission requirement, the formation must remain rigid during the nominal mission operations, hence the relative positions and orientations of the satellites to each other must remain fixed. This condition is obtained imposing a forced relative motion. The satellites are equipped with low-thrust engines, which provides a continuous control force. This contribution can be easily introduced in the Hill-Clohessy-Wiltshire equations of motion[11]. The general solution of the HCW forced motion reads:

$$
\begin{aligned}
z[t] =& \frac{1}{n^2}\Big(C_z - C_z cos(nt) + n^2 z_0 cos(nt) + \\
&+ n\, z_0' sin(nt)\Big) \\
x[t] =& \frac{1}{n^2}\Big(C_x + 2n(C_y\, t + 2\, n\, x_0 + y_0') + \\
&- (C_x + + n(3\, n\, x_0 + 2 y_0'))cos(nt) + \\
&+ (n\, x_0' - 2C_y) sin(nt)\Big) \\
y[t] =& \frac{1}{2n^2}\Big(C_y(8 - 3n^2 t^2) - 2n(2C_x t + 2x_0' + \\
&+ n(6\, n\, t\, x_o - y_0 + 3\, t\, y_0')) + \\
&+ (4n\, x_0' - 8C_y) cos(nt) + \\
&+ 4(C_x + n(3\, n\, x_0 + 2\, y_0')) sin(nt)\Big)
\end{aligned}
\qquad [3]
$$

From the general solution we impose that the general relative state in time $x[t],\ y[t],\ z[t]$ remain equal to the initial conditions x_0, y_0, z_0 at any time instant. We also impose that at $t = 0$, the relative velocity component is null: $x_0' = y_0' = z_0' = 0$. This allows to recover the acceleration components C_x, C_y, C_z necessary to maintain a constant relative position among the satellites:

$$\begin{aligned} C_x &= -3n^2 x_0 \\ C_y &= 0 \\ C_z &= n^2 z_0 \end{aligned} \qquad [4]$$

Now, from the acceleration components, the delta-v required by the forced motion over one orbit period is evaluated multiplying the acceleration values times the orbital period. The analysis is performed for four different formation geometries:

i. Formation with $\gamma = 0°$ or $180°$ (FF-B2).
ii. Formation with $\gamma = 90°$ or $270°$ (FF-B1).
iii. Formation with $\gamma = 90°$ or $270°$ and a normal displacement $\Delta N = 1.875$ m.
iv. Formation with $\gamma = 90°$ or $270°$ and both a normal and a radial displacement: $\Delta N = 1.875$ m and $\Delta R = 3$ m.

The results of these analyses are reported in Fig. X. It is shown how the first case is completely unbalanced, as satellite A requires no delta-v to maintain the initial relative state. On the other hand, the fourth case, representing the R-displaced condition, requires the highest delta-v for the forced motion. Finally, the third case is preferred over the second one, resulting in a completely balanced scenario. The N-displaced condition assures an equal delta-v budget among the satellites for the nominal operations. Moreover, it is a good trade-off among the delta-v required in case ii: the propellant consumption less than the maximum of satellite A in case ii and slightly higher than the values for the other two satellites B and C.

Thus, this second analysis set the formation configuration with a N-displacement of 1.875 m and a preferred $\gamma = 270°$.

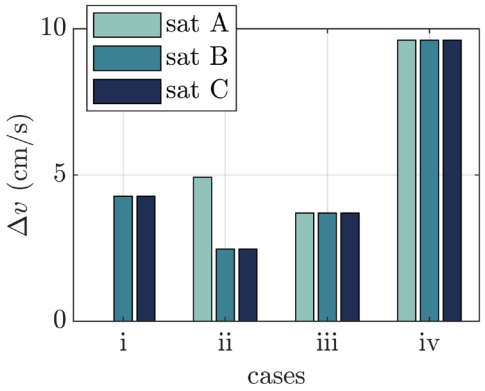

Fig. X: Delta-v computation over one orbital period for each satellite under the four cases under analysis.

IV.III Sun Analysis and shadowing effect

A proper analysis on the Sun direction is an important factor for the selection of the mission operations of the formation. The solar panels are placed only on the Sun-faced sides of each satellites. Moreover, the close inter-satellite distance, just 13 m among the central point of each satellite, as in Fig. II, requires a further analysis on the possible self-shadowing effect. The aim of the analysis is to define the best formation configuration to minimise the possible self-shadowing effect, in terms of the γ angle. The illumination factor shows that the configuration, with a yaw angle of $\gamma = 90°$ or $270°$, minimises the self-shadowing effect, as in Fig. XI.

Moreover, the β angle between the normal direction (N) and the Satellite-Sun vector is evaluated over 1-year period, starting from the Spring equinox. Consequently, the power budget is designed consistently with the seasonal variation of the β angle and the orbital variation of the elevation angle. The latter is the angle formed among the normal to the solar panel and the Sun direction. The maximum oscillation condition arises at the winter solstice, according to the β angle, as shown in Fig. XII. Thus, from this analysis it is confirmed the preference for a yaw angle of $\gamma = 270°$, to minimise the self-shadowing effect.

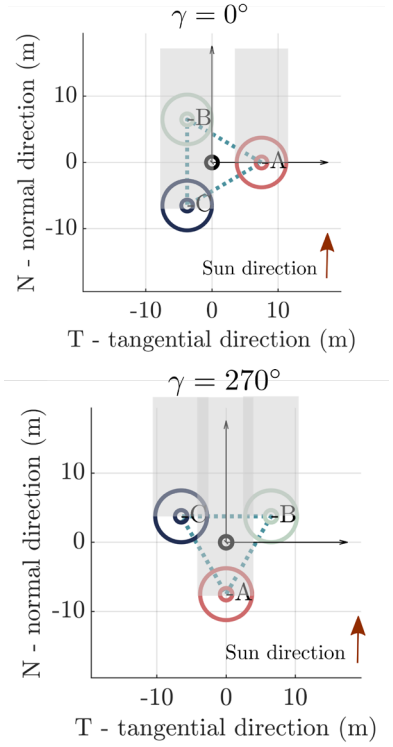

Fig. XI: Self-shadowing effect for the formation configuration with $\gamma = 0°$ (top) and $\gamma = 270°$ (bottom). The shadowing is depicted in light grey, consistently with the Sun direction.

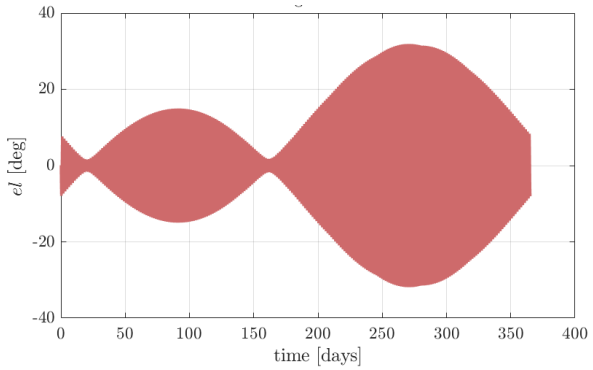

Fig. XII: Solar elevation angle in the RTN frame, among the solar panel normal and the sun-satellite direction.

IV.IV Plume impingement analysis

The satellites in the formation are equipped with low thrust engine. The analysis of the plume impingement is important to provide a preliminary study on the side effect of a low thrust plume on the satellite's equipment. Specifically, the plume is made by an ion beam, which can be modelled as a cone defined by the exit velocity and the yaw angle of the engine[14,15].

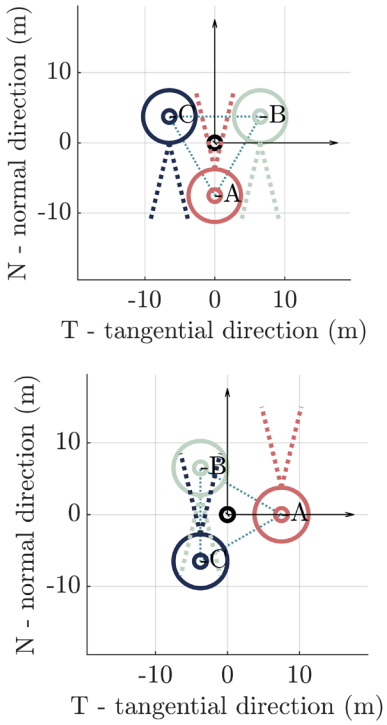

Fig. XIII: Plume impingement analysis for $\gamma = 0°$ (left) and $\gamma = 270°$ (right). The plume ejecta is represented with the dot lines for each satellite.

The analysis is performed considering a maximum available thrust of 5 mN to counteract the natural oscillatory motion. From the natural dynamic analysis, Eq. [4], an acceleration of the order of $7 \cdot 10^{-6}$ m/s^2 is required in the normal (N) direction. Thus, considering a formation with null radial displacement, two cases are analysed: $\gamma = 0°$ and $\gamma = 270°$, as in Fig. XIII. These two situations represent the two extreme conditions to be analysed. In the former one, the plume cone of satellite B and C completely interfere with the satellite body, causing potential harness to the electronics and optical instruments. The latter, instead, provides a more favourable situations, avoiding the direct impingement of the plume on the satellites body.

Consequently, this final analysis confirms the advantages of selecting a yaw angle of 270° for the formation during the nominal mission operations.

V. FINAL SELECTION OF THE FORMATION GEOMETRY

From the analyses in Section IV, the following baseline formation is finally identified:

i. Yaw angle $\gamma = 270°$.
ii. R- and N-displaced orbit: $\Delta R = 0$ m and $\Delta N = 1.875$ m.
iii. Initial argument of latitude: $u_0 = 0°$ or $180°$.

This provides the best situations in terms of ROEs natural evolution, propellant balance for the δN displacement, plume impingement analysis and self-shadowing effect.

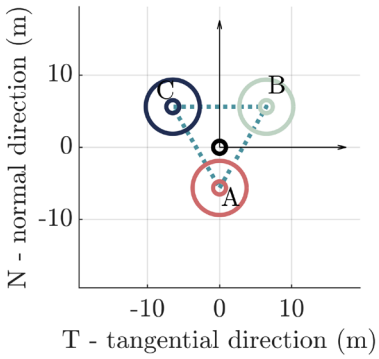

Fig. XIV: Final selection of the formation configuration for the L-band aperture synthesis mission.

VI. CONSIDERATIONS ON THE FORMATION SAFETY

The inter-satellite collision risk for the formation is evaluated over one orbital period, for the un-controlled propagation. Thus, the relative dynamics is not forced by the continuous control thrust and the relative positions evolves under the effect of the mean J_2 perturbation. Two

quantities are evaluated to assess the inter-satellite collision risk.

First, the three-dimensional distance among each couple of satellites in the RTN frame is evaluated. For the analysis, an initial argument of latitude at the ascending node is considered for the formation: $u_0 = 0°$. The satellites are designed to have a polygonal shape, for the L-band interferometer, with an external diameter of 7.5 m. For this reason, if the 3D distance is less than two times the satellite radius, margined by 20%, there is a collision among the spacecraft: 7.5 m + 20%. Due to the mission scientific requirements, the equilateral triangle defining the formation geometry must remain fixed during the scientific operations. Thus, the evaluation of the 3D inter-satellite distance provides the same results for the baseline, the N-displaced and the R-displaced formation. As shown in Fig. XV, the natural motion of the formation is not sustainable since it results in the collision of at least the satellites just in one orbit.

Moreover, a second analysis is performed. The two-dimensional inter-satellite distance is evaluated in the radial-normal (RN) plane. This provides information on the separation in the radial-normal plane and, therefore, on the eccentricity/inclination vector passive safety. For this analysis, a lower limit for the collision is set at 7.5 m + 20% margin.

The results are shown in Fig. XVI. For an un-controlled motion, the 2D distance violates the collision limit in one orbital period, as for the 3D study. Consequently, the following considerations are valid:

i. The satellites should remain fixed at the vertex of the equilateral triangle during nominal operations: fixed and rigid formation.
ii. The formation must fly under a continuously forced motion, to control accurately the relative satellite position at any time instant.
iii. A robust formation safety policy should be implemented to minimise the inter-satellite collision risk in case of a failure of the on-board engine.

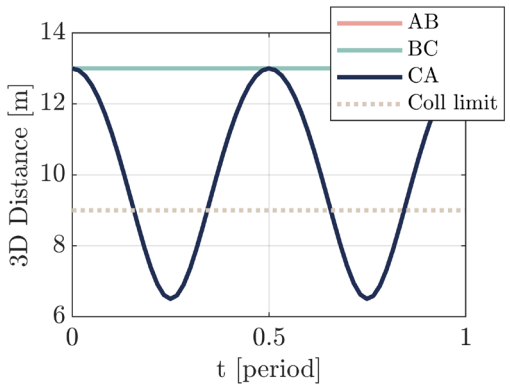

Fig. XV: Three-dimensional inter-satellite distance in the RTN space for $\gamma = 270°$. The collision limit is considered 7.5 m + 20% margin.

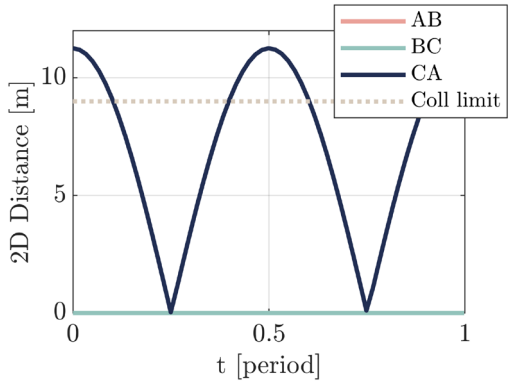

Fig. XVI: Two-dimensional inter-satellite distance in the RN plane, for $\gamma = 270°$. The collision limit is considered 7.5 m + 20% margin.

VI. CONCLUSIONS

In this paper, we show the approach to design the operational geometry for a three-satellite formation for Earth observation purposes. The aim of the study is to identify a couple of yaw angle γ and initial argument of latitude u_0, which minimise the control effort in terms of delta-v, the plume impingement and the self-shadowing effect. The analysis is carried out considering that the relative position among the satellites should remain fixed for the whole operative phase, due mission requirement on the intersatellite optical link.

Section IV. shows the importance of initialise the formation at the nodes of the reference orbit. An initial argument of latitude of $0°$ or $180°$ reduces the effect of the mean J_2 on the natural evolution of the relative orbital elements of the satellites. Moreover, a detailed analysis on the possibility to exploit normal and radial displaced orbits is carried out. The advantage of N-displaced orbits is evaluated in terms of delta-v budget for the three satellites. This effect is combined with the yaw angle of the formation, γ, which identifies the orientation of the equilateral triangle in the transversal-normal plane. A ΔN of $1.875\ m$ together with a $\gamma = 270°$ allows an equal delta-v for each satellite during the nominal operation of the formation. This is of primary importance for the design of the satellite platform: a balance in terms of propellant consumption allows an equal platform design for the formation. The advantage of a yaw angle of $\gamma = 270°$ is confirmed by the analysis on the self-shadowing effect and the plume impingement. The former ensures the proper power generation of the solar panels. On the other hand, the ion plume impingement could damage or deteriorate the external devices of a satellites. Thus, it is important to provide an initial formation geometry, which could reduce and minimise such effect.

Finally, an overview on the safety condition of the formation in terms of inter-satellite collision risk is

provided. These preliminary analyses on the formation flying geometry selection will be integrated with further analysis on the intersatellite collision risk strategies. A detailed procedure to implement the safe mode on-board the satellite will be implemented in future development of the project.

VII. ACKNOLEDGMENT

The project presented in this paper was carried out as part of the European Space Agency Contract (Contract No. 4000128576/19). The view expressed in this paper can in no way be taken to reflect the official opinion of the European Space Agency.

The work was co-founded by the European Space Agency (Contract No. 4000128576/19) and by the European Research Council (ERC) under the European Union's Horizon 2020 research and innovation program (grant agreement No. 679086 COMPASS).

The contribution of Dr. Gabriella Gaias is funded by the European Union's Horizon 2020 research and innovation program under the Marie-Sklodowska Curie grant ReMoVE (grant agreement No.793361).

The authors acknowledge the contribution of Berthyl Duesmann and Itziar Barat, orbital experts at ESA European Space Research and Technology Centre (ESTEC).

The authors also would like to acknowledge Miguel Piera's support, from Airbus Space España, leading the contract.

[1] Kerr, Y. H., Waldteufel, P., Wigneron, J. P., Martinuzzi, J. A. M. J., Font, J., & Berger, M. (2001). Soil moisture retrieval from space: The Soil Moisture and Ocean Salinity (SMOS) mission. IEEE transactions on Geoscience and remote sensing, 39(8), 1729-1735.

[2] Kerr, Y. H., Al-Yaari, A., Rodriguez-Fernandez, N., Parrens, M., Molero, B., Leroux, D., ... & Delwart, S. (2016). Overview of SMOS performance in terms of global soil moisture monitoring after six years in operation. Remote Sensing of Environment, 180, 40-63.

[3] Krieger, G., Moreira, A., Fiedler, H., Hajnsek, I., Werner, M., Younis, M., & Zink, M. (2007). TanDEM-X: A satellite formation for high-resolution SAR interferometry. IEEE Transactions on Geoscience and Remote Sensing, 45(11), 3317-3341.

[4] Moreira, A., Krieger, G., Hajnsek, I., Papathanassiou, K., Younis, M., Lopez-Dekker, P., ... & De Zan, F. (2015). Tandem-L: A highly innovative bistatic SAR mission for global observation of dynamic processes on the Earth's surface. IEEE Geoscience and Remote Sensing Magazine, 3(2), 8-23.

[5] M. Martin-Neira, A. M. Zurita, M. A. Plaza, and F. J. Benito, "SMOS Follow-on Operational Mission Concept (SMOSops-H)," 2nd SMOS Science Conference, ESAC, Villanueva de la Canada, 25-29 May 2015.

[6] Scala, F., Gaias, G. V. M., Colombo, C., & Martin Neira, M. (2020). Three Satellites Formation Flying: Deployment and Formation Acquisition Using Relative Orbital Elements. In 2020 AAS/AIAA Astrodynamics Specialist Conference (pp. 1-17).

[7] Gaias, G., Ardaens, J. S., & Montenbruck, O. (2015). Model of J_2 perturbed satellite relative motion with time-varying differential drag. Celestial Mechanics and Dynamical Astronomy, 123(4), 411-433.

[8] D'Amico, S. (2005). Relative orbital elements as integration constants of Hill's equations. DLR, TN, 05-08.

[9] Gaias, G. V. M., & Colombo, C. (2018). Semi-analytical framework for precise relative motion in low earth orbits. In 7th International Conference on Astrodynamics Tools and Techniques (ICATT) (pp. 1-10).

[10] Drinkwater, M. R., Haagmans, R., Muzi, D., Popescu, A., Floberghagen, R., Kern, M., & Fehringer, M. (2006, November). The GOCE gravity mission: ESA's first core Earth explorer. In Proceedings of the 3rd international GOCE user workshop (pp. 6-8). Noordwijk, The Netherlands: European Space Agency.

[11] Clohessy, W. H., & Wiltshire, R. S. (1960). Terminal guidance system for satellite rendezvous. Journal of the Aerospace Sciences, 27(9), 653-658.

[12] Curtis, H. D. (2013). Orbital mechanics for engineering students. Butterworth-Heinemann.

[13] Vallado, D. A. (2001). Fundamentals of astrodynamics and applications (Vol. 12). Springer Science & Business Media.

[14] Bombardelli, C., & Pelaez, J. (2011). Ion beam shepherd for contactless space debris removal. Journal of guidance, control, and dynamics, 34(3), 916-920.

[15] Roberts, C., & Hastings, D. (2002). Electric thruster impingement effects on multiple spacecraft system environments. In 38th AIAA/ASME/SAE/ASEE Joint Propulsion Conference & Exhibit (p. 3670).